



Perspectives on Magnetar Burst Emission

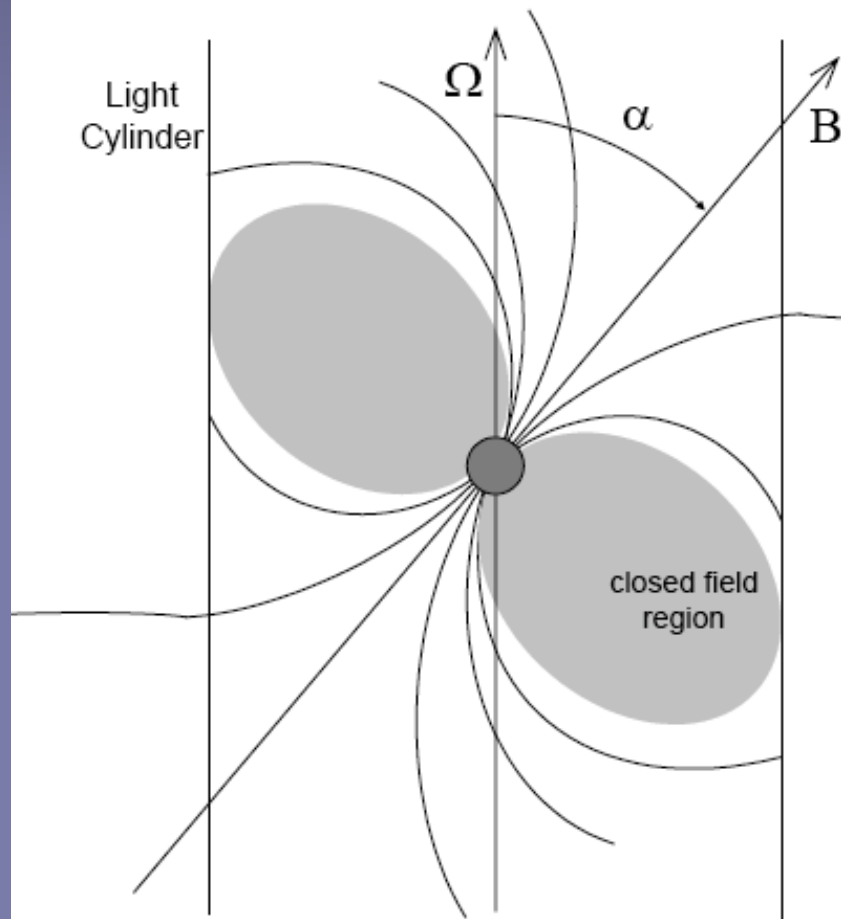
Matthew G. Baring
Rice University

Annapolis GRB meeting, 3rd November, 2010

And now for something completely different – Magnetars!

- Neutron stars, with vengeance: a snapshot of flare observations;
- Energetics => high Thomson opacity;
- Resonant Compton physics;
- Magnetic pair creation $\gamma \rightarrow e^+e^-$ and photon splitting $\gamma \rightarrow \gamma \gamma$: variations on the theme;
- Future directions: hard X-ray telescopes and Compton polarimetry?

Rotating dipole model



- **Magnetic dipole radiation**

$$\dot{E}_{SD} = -\frac{B_0^2 \sin \alpha \Omega^4 R^6}{6c^3} = I\Omega\dot{\Omega}$$

- **Braking index**

$$\dot{\Omega} = -K\Omega^n \quad n = \frac{\ddot{\Omega}\Omega}{(\dot{\Omega})^2} = 3$$

- **Surface B field**

$$B_0 = \left(\frac{3Ic^3 P\dot{P}}{2\pi^2 R^6} \right)^{1/2}$$

- **Characteristic age**

$$\tau \approx \frac{-\Omega}{(n-1)\dot{\Omega}} = \frac{P}{2\dot{P}}$$

Magnetars: Pulsars with $B \sim 10^{14}$ - 10^{15} Gauss!

- Neutron stars with abnormally high fields: periods $P=2$ - 12 seconds, with rapid spin-down.
- Magnetar concept proposed by Duncan & Thompson.
- **Two varieties:**
- **Anomalous X-ray Pulsars** (AXPs): known for decades, and spin-down steadily; luminosities ($L_x \sim 10^{35}$ erg/sec) are **too bright and spin periods generally too short** for accreting neutron star systems;
- **Soft Gamma Repeaters** (SGRs) were discovered around 1979 (then thought to be gamma-ray bursts), and possess flaring activity, with sometimes **phenomenal outbursts** ($L \sim 10^{42}$ - 10^{46} erg/sec = **highly super-Eddington**) **displaying periodicity**;
- **Both** display quiescent X-ray emission of both thermal and non-thermal origins.
- **Both** display flare activity (e.g. see van de Horst talk on SGR 1550/AXP 1E 1547), **but only SGRs exhibit giant flares.**

SGR 0525-66 Mar. 5th 1979 Event Time History

70

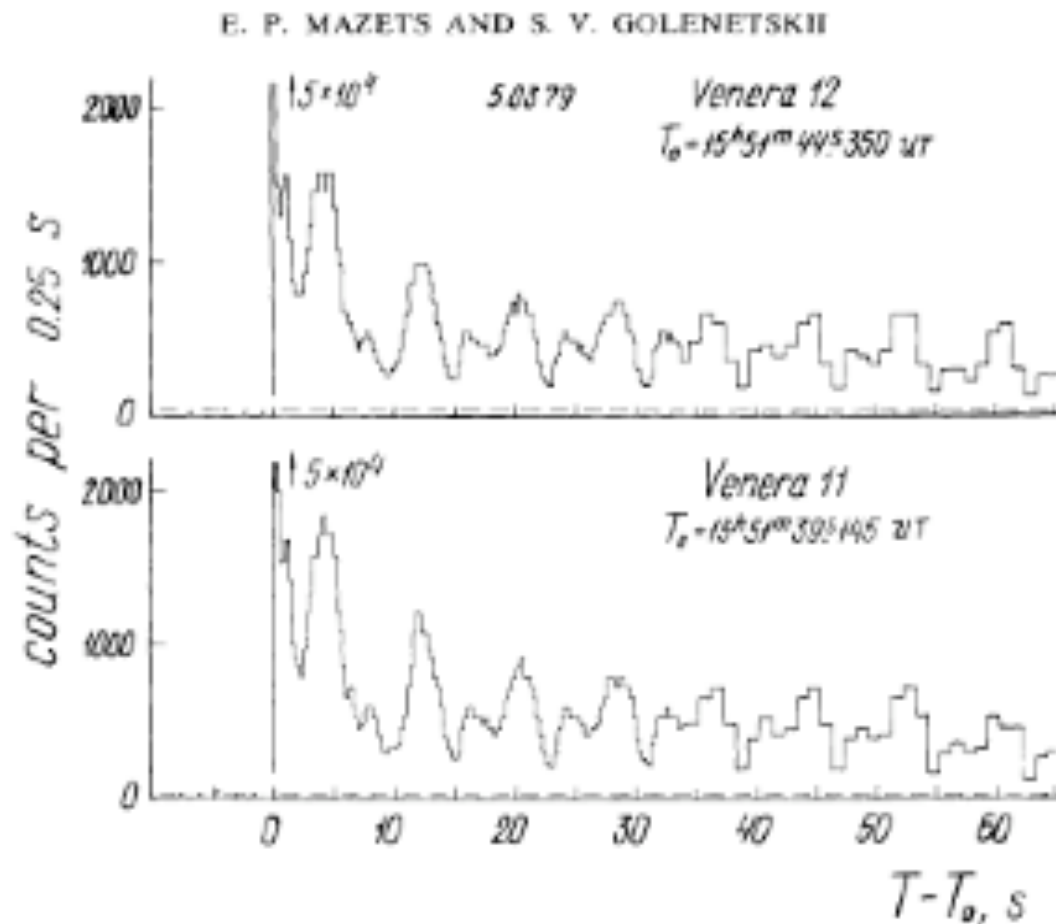
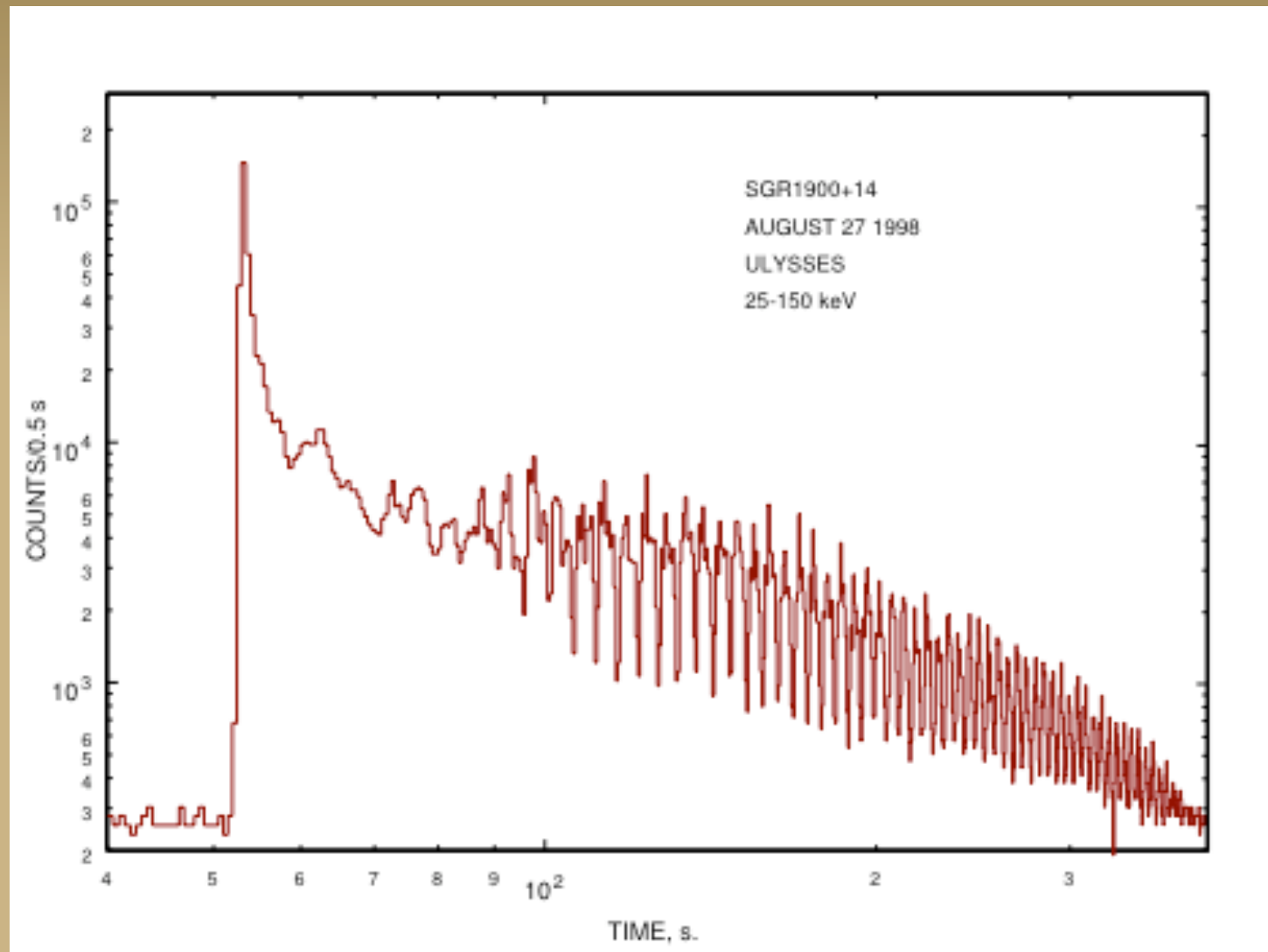


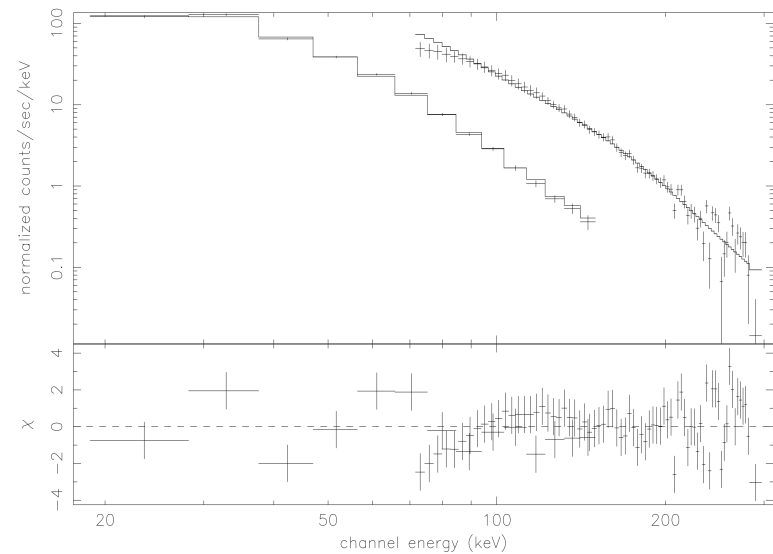
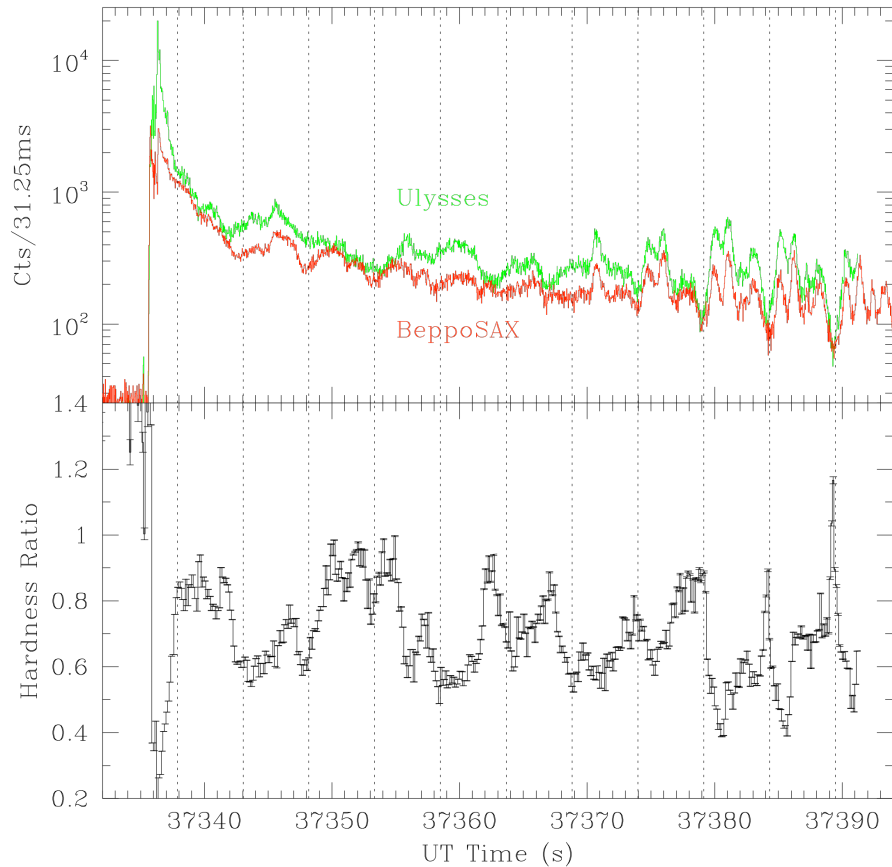
Fig. 23. The time profile of the 5 March, 1979 event recorded with a resolution of 0.25 s (at the end of recording, with 1 s resolution). The background level is shown by a dashed line.

SGR1900+14 Giant Flare Lightcurve



Source: Kevin Hurley

SGR 1900+14 Giant Flare Tail



- Feroci et al. ApJ 2001;
- 2xBB or OTTB @ 20-30 keV
+ PL @ index $\sim 2.7-3.4$

SGR 1900+14 Outburst light curves and spectrum (Jun-Aug 1992)

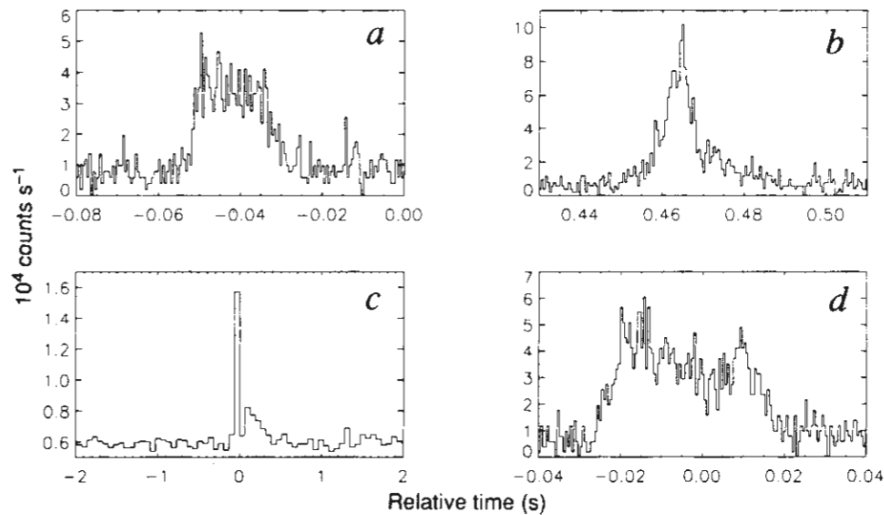


FIG. 1 Light curves of the three SGR bursts detected with the Burst and Transient Source Experiment (BATSE) on the Compton Gamma Ray Observatory. BATSE is unique in combining good sensitivity to weak γ -ray and SGR-like bursts with the capability of determining their locations in a single experiment. *a, b*, First and second pulse, respectively, of the 19 June 1992 trigger. The counts are integrated between 20 and 100 keV. Time resolution is 0.512 ms. *c*, Event of 8 July 1992 recorded with 64-ms time resolution (the only resolution available). The initial spike of <64 ms appears only up to 100 keV. *d*, Event of 19 August 1992 recorded with 0.512-ms resolution between 20 and 100 keV. Notice the similarity in structure between *a* and *d*.

NATURE · VOL 362 · 22 APRIL 1993

■ Kouveliotou et al. (1993)

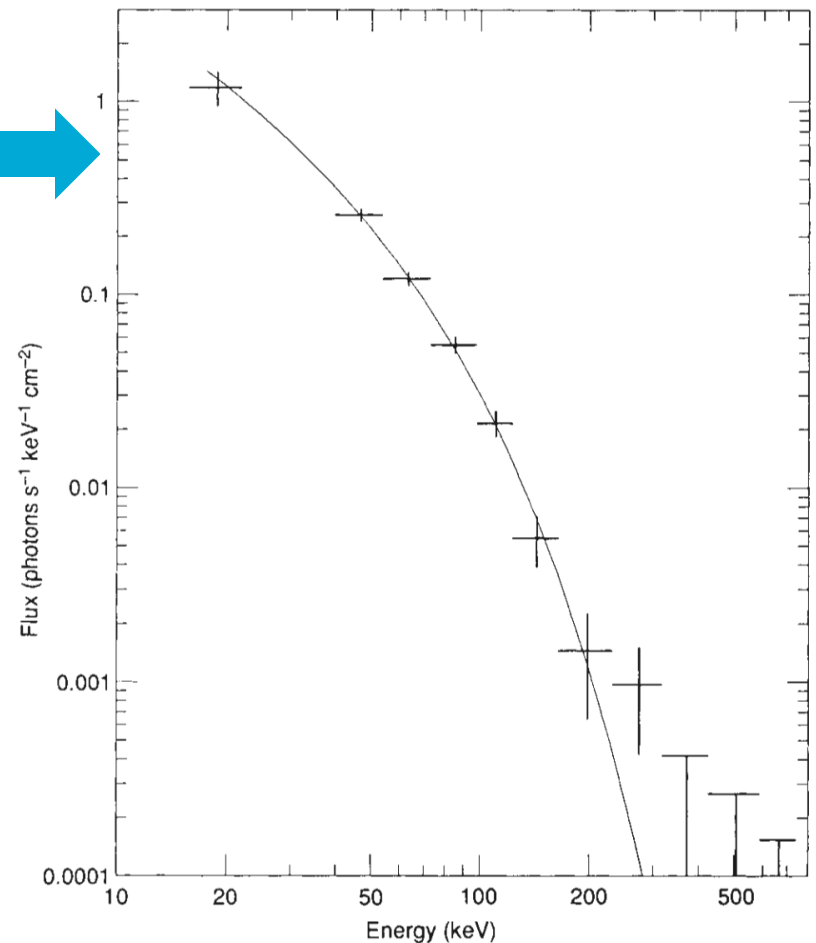


FIG. 2 Photon spectrum of the pulse of Fig. 1*b*. The spectrum is integrated over 32 ms and corresponds to the peak of the pulse. The gap in the spectrum between ~ 20 and 40 keV is due to a period of telemetry failure during transmission of the data. The curve indicates the best-fit OTTB function, of the form $A \exp(-E/KT)/E$, with $kT = 39 \pm 3$ keV.

Duncan & Thompson magnetar flare model

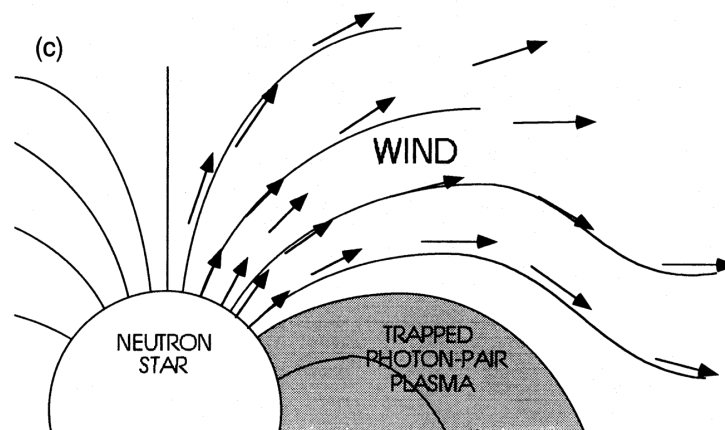


Figure 1. (c) Not all the energy can be contained by the magnetosphere at radius R_m , unless the total energy released is a very small fraction of the dipole magnetic energy of the star. As a result, the pressure of the photon-pair plasma drives a wind from the magnetosphere. This probably occurred in the 1979 March 5 event, but probably not in most ordinary SGR events.

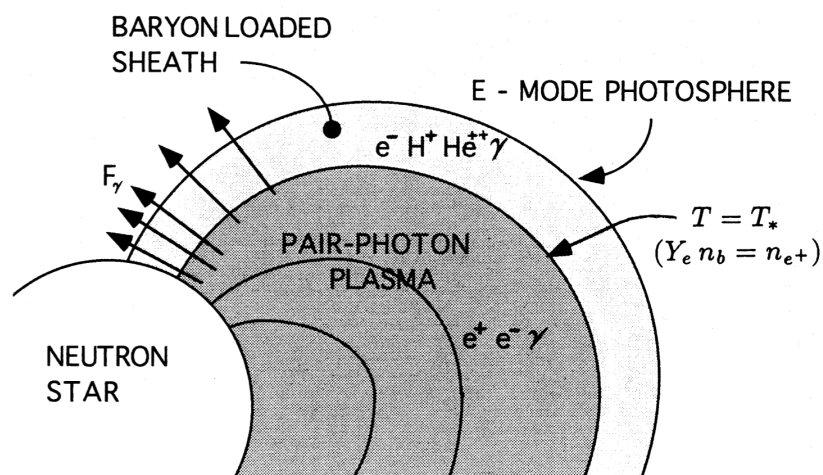


Figure 2. The deposition of $\geq 10^{38}$ – 10^{41} erg in the magnetosphere of a neutron star is sufficient to generate an optically thick photon–electron–positron plasma. The surface of this plasma is congruent with the magnetic field lines. The surface layers lose heat by radiative diffusion, and the scattering opacity in these layers is dominated by a small contaminant of ions and electrons blown off the neutron star surface.

Magnetar Flare Energetics

- **Energetics** of magnetar flare emission **constrains the electron number density** n_e . Let $\langle \gamma_e \rangle$ be their mean Lorentz factor, and ϵ_{rad} their radiative efficiency. Then

$$L_{X\gamma} \sim \epsilon_{\text{rad}} \langle \gamma_e \rangle m_e c^2 (4\pi n_e R_c^2 c)$$

This yields $n_e \sim 3 \times 10^{22} L_{X\gamma,42} / \epsilon_{\text{rad}} \langle \gamma_e \rangle \text{ cm}^{-3}$ for scaled luminosities $L_{X\gamma,42} \equiv L_{X\gamma} / 10^{42} \text{ erg/sec}$, if $R_c \sim 10^7 \text{ cm}$.

- The Thomson optical depth is (for $R_c = 10^6 R_6 \text{ cm}$)

$$\tau_T \sim \frac{2 \times 10^4 L_{X\gamma,42}}{\epsilon_{\text{rad}} \langle \gamma_e \rangle R_6}$$

- Comparing n_e to the classic Goldreich-Julian (1969) density $n_{\text{GJ}} = \nabla \cdot \vec{E} / 4\pi$ gives

$$\frac{n_e}{n_{\text{GJ}}} \approx \frac{4.7 \times 10^{10} L_{X\gamma,42} P}{\epsilon_{\text{rad}} \langle \gamma_e \rangle B_{15} R_6^2}$$

- **Requisite density is highly super-Goldreich-Julian.**

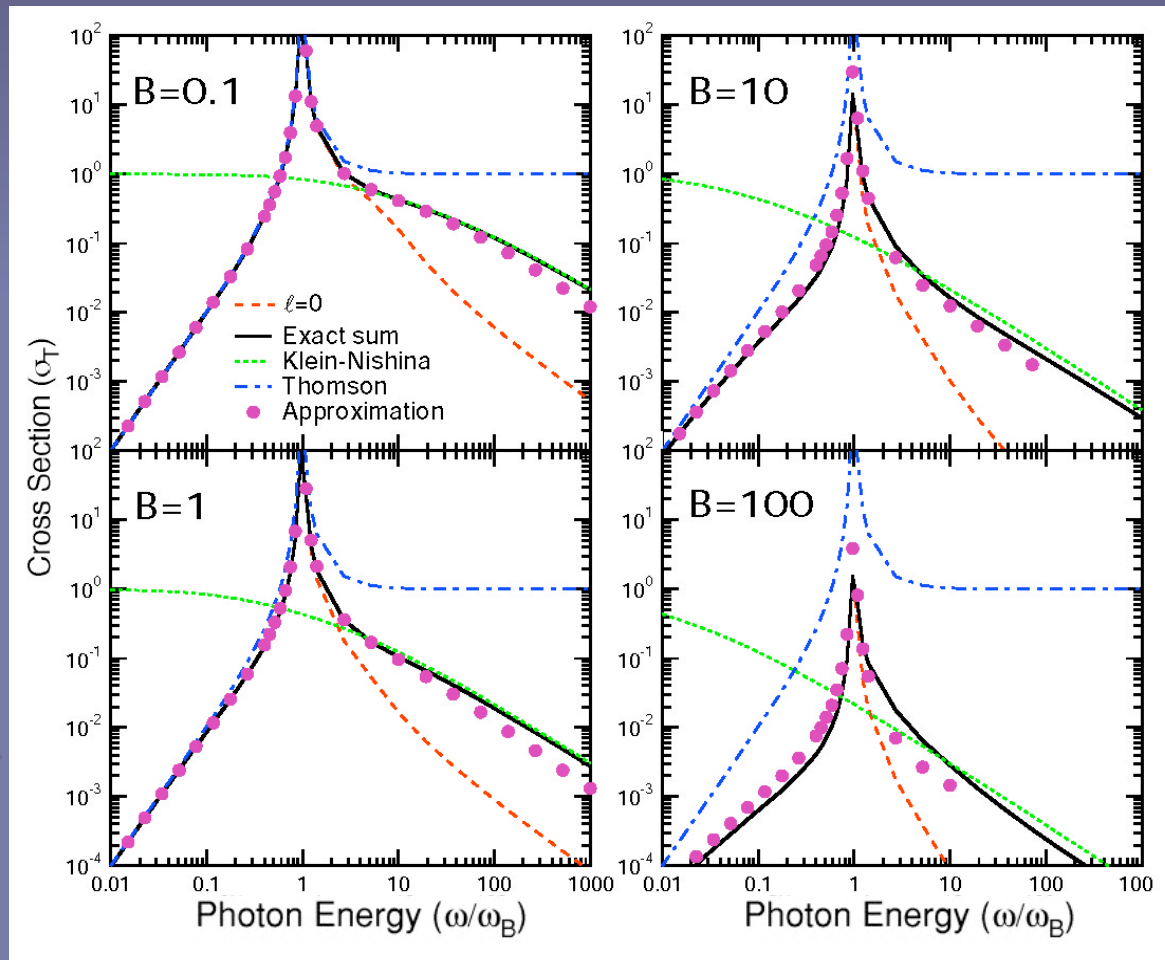
* \Rightarrow classic pulsar mode cannot work for magnetar flares

Resonant Compton Cross Section

- Illustrated for photon propagation **along B**;
- In magnetar fields, cross section declines due to Klein-Nishina reductions;
- Resonance at cyclotron frequency $eB/m_e c$;
- Below resonance, $l=0$ provides contribution;
- In resonance, cyclotron decay width truncates divergence.

$B=1 \Rightarrow B=4.41 \times 10^{13} \text{G}$

Gonthier et al. 2000



Process becomes effectively first order in the fine structure constant: the virtual electron behaves like a real one in the first excited state and spawns cyclotronic decay.

Resonant Thomson Cross Section

- Cross section in strong B fields is strongly-suppressed below the cyclotron resonance $\omega_B = B$ for photons beamed along \vec{B} .

$$\sigma_{\perp \rightarrow \perp} = \frac{3\sigma_T}{8} \left\{ \left(\frac{\omega}{\omega + \omega_B} \right)^2 + \left(\frac{\omega}{\omega - \omega_B} \right)^2 \right\} ,$$

$$\sigma_{\perp \rightarrow \parallel} = \frac{\sigma_T}{8} \left\{ \left(\frac{\omega}{\omega + \omega_B} \right)^2 + \left(\frac{\omega}{\omega - \omega_B} \right)^2 \right\} ,$$

$$\sigma_{\parallel \rightarrow \perp} = \frac{3\sigma_T}{8} \cos^2 \theta_i \left\{ \left(\frac{\omega}{\omega + \omega_B} \right)^2 + \left(\frac{\omega}{\omega - \omega_B} \right)^2 \right\} ,$$

$$\sigma_{\parallel \rightarrow \parallel} = \sigma_T \sin^2 \theta_i + \frac{\sigma_T}{8} \cos^2 \theta_i \left\{ \left(\frac{\omega}{\omega + \omega_B} \right)^2 + \left(\frac{\omega}{\omega - \omega_B} \right)^2 \right\} .$$

- **Equatorial magnetospheric locales:** If $\theta_i \sim \pi/2$, **attenuation lengths are widely disparate between polarization modes.**
- **Polar magnetospheric locales:** If relativistic boosting due to electron motion along B sets $\theta_i \approx 0$ in the electron rest frame, then in Thomson regime, $\sigma_{x \rightarrow \perp} / \sigma_{x \rightarrow \parallel} = 3$.
- **Emission will display strongly angle-dependent polarization.**

Compton Scattering Mode Conversion and Eddington Luminosity

- L_{edd} in parallel mode is nominally $1.4 \times 10^{38} (B/\omega)^2$ for transport along B (e.g. Ulmer 1994);
- Miller (1995) noted that polarization mode conversion par- \rightarrow perp would reduce this by factor of ω/B .
- Generates L_{edd} in photospheric equatorial bubbles.
- Perp mode dominates polarization, and more so at lower energies.

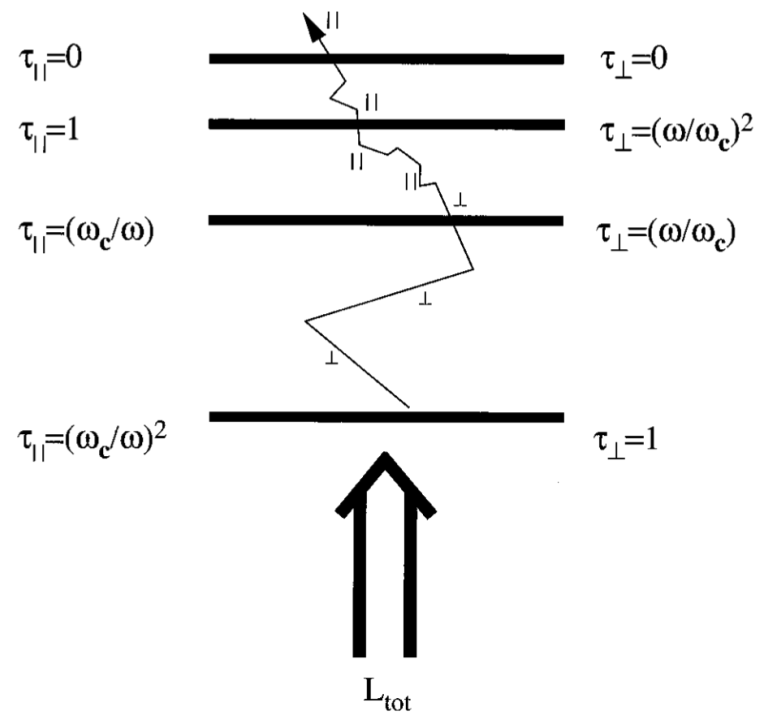


FIG. 1.—Schematic diagram of photon propagation through an atmosphere. A total luminosity L_{tot} is released deep in the atmosphere at a perpendicular optical depth $\tau_{\perp} \gg 1$. It then scatters many times, occasionally changing polarization, until it finally escapes. The sample photon represented in this figure converted from perpendicular to parallel at $\tau_{\parallel} < (\omega_c/\omega)$ and was still in the parallel mode when it escaped.

Feynman Diagrams

Conversion
of photons
into pairs

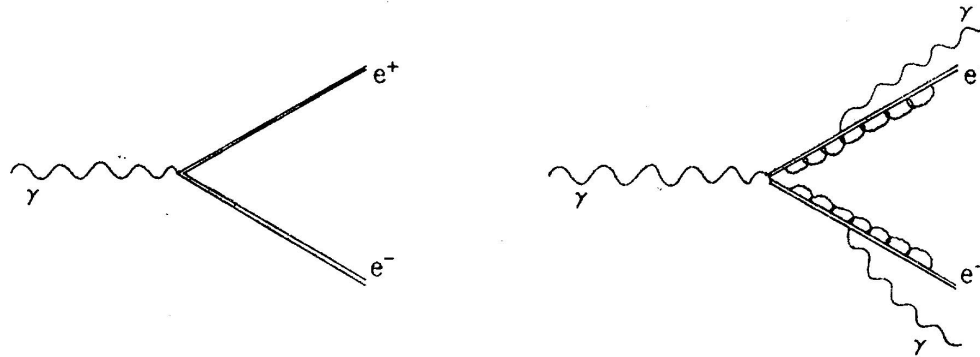


FIG. 1. (a) Pair production in a moderately strong field. The double lines denote the binding effects. (b) Pair production in a strong field. The bound propagators are modified by virtual photon (radiation reaction) loops.

Splitting of
photons in
two

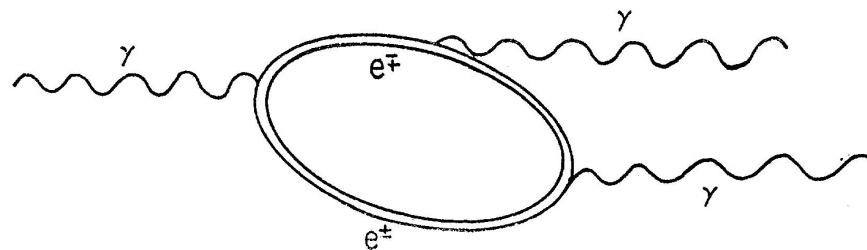


FIG. 2. Photon splitting in a strong field. One of the intermediate particles in a vacuum polarization loop emits a photon.

■ (From Erber 1966)

Single Photon Pair Creation

- $\gamma \rightarrow e^+e^-$ occurs only in strong E/M fields where momentum conservation is not imposed perpendicular to \mathbf{B} :

$$B \sim B_{\text{cr}} \equiv \frac{m_e^2 c^3}{e\hbar} = 4.413 \times 10^{13} \text{ Gauss} \quad .$$

($B = B_{\text{cr}} \Rightarrow$ cyclotron energy equals $m_e c^2$).

- As a gamma-ray attenuation mechanism, it is strongly polarized, with a higher threshold for the \perp state:

$$\parallel: \quad \omega \geq \frac{2m_e c^2}{\sin \theta_{kB}} \quad , \quad \perp: \quad \omega \geq \left(1 + \sqrt{1 + 2B/B_{\text{cr}}}\right) \frac{m_e c^2}{\sin \theta_{kB}} \quad .$$

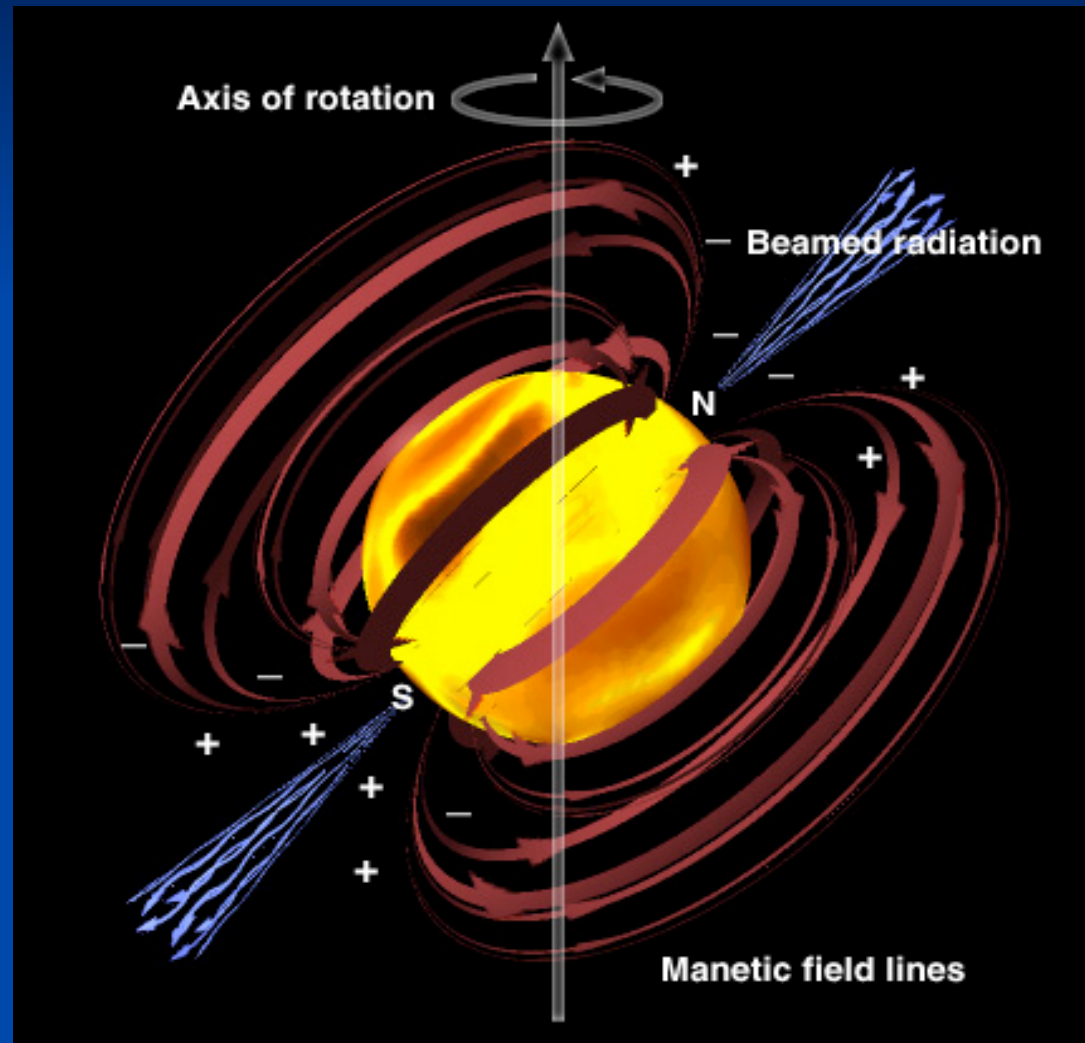
- Continuum asymptotic expressions for rates (Erber 1966; Tsai & Erber 1974) for subcritical fields yield

$$\frac{R_{\parallel}}{R_{\perp}} = 2 \quad , \quad R_{\parallel} + R_{\perp} \propto B \sin \theta_{kB} \exp\left\{-\frac{8m_e c^2 B_{\text{cr}}}{3\omega B \sin \theta_{kB}}\right\} \quad .$$

Pairs: where are they?

- Presence of pairs enhances radiative efficiency, but reduces Eddington luminosity (circumvented by field trapping);
- Pair abundance in giant flare tails or moderate flares is exponentially suppressed since $T/m_e c^2 \ll 1$;
- Pair annihilation timescale is short, $< 10^{-4}$ sec;
- Tail emission is below $\gamma \rightarrow e^+e^-$ threshold;
- Pair creation can proceed in giant flare initial spikes. Photons spill over to closed field regions not particularly efficient.
- Pair prod. seeded by E-field sparking / discharge (Beloborodov '07)
- If $T/m_e c^2 \gg 1$ plasma starts out deep inside equatorial "photosphere," reprocessing by pair creation and photon splitting can degrade spectrum $T/m_e c^2 < 0.1$.

Outflow/jet + equatorial bubble geometry for SGR giant (XXX class) flares:



Magnetic Photon Splitting

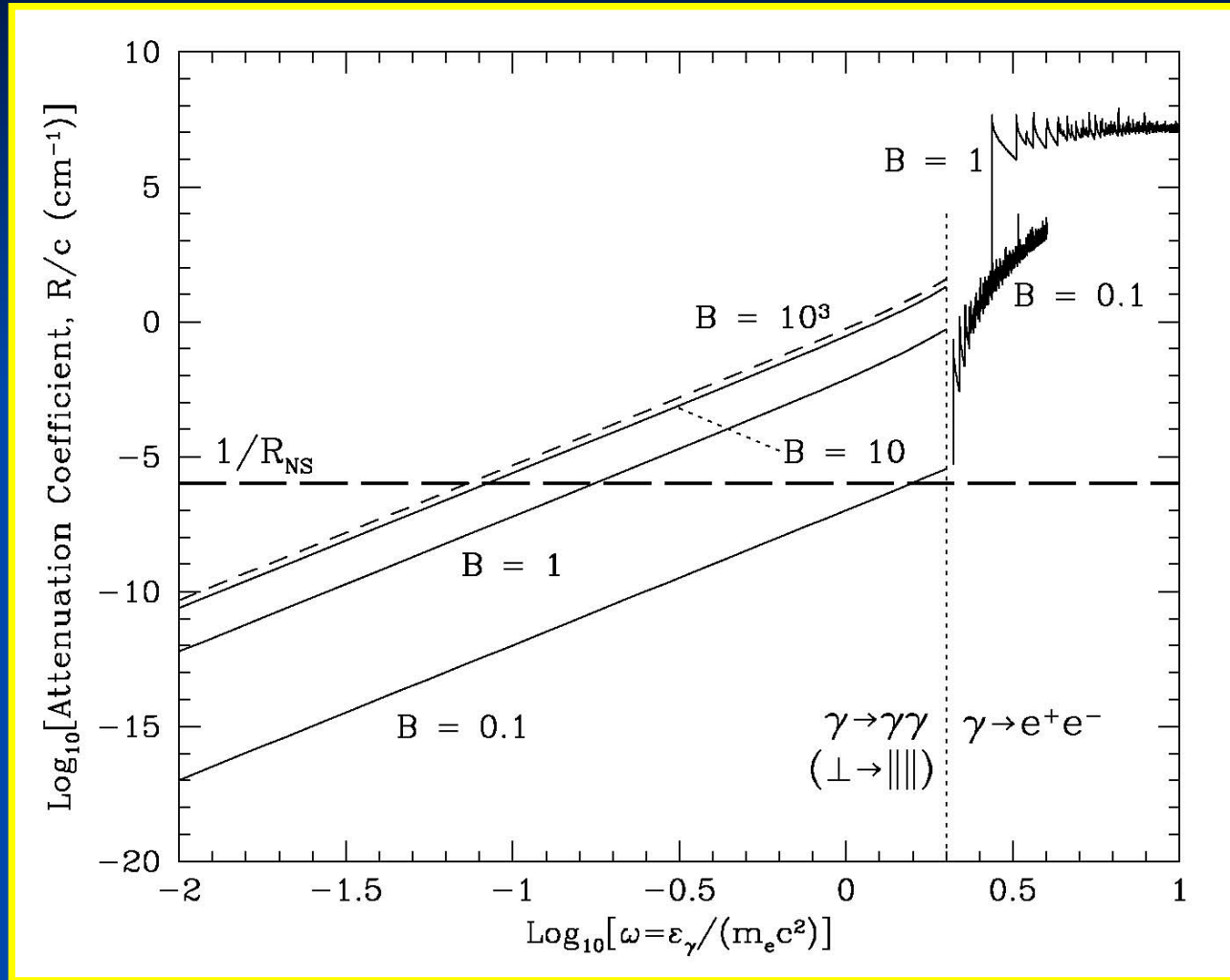
- $\gamma \rightarrow \gamma\gamma$ is another truly quantum process that for $B \gtrsim 3 \times 10^{13}$ G can compete with pair creation as an attenuation process;
 - * when $B = 0$, it is forbidden by Furry's theorem due to charge symmetry of electron/positron propagators.
- In QED, 3 polarization modes yield non-zero amplitudes \mathcal{M} in the absence of dispersion:

$$\perp \rightarrow \parallel\parallel \quad , \quad \perp \rightarrow \perp\perp \quad , \quad \parallel \rightarrow \perp\parallel \quad .$$

Rates are proportional to $\omega^5 (\mathcal{M})^2$ for $\omega \ll 1$, and depend on the polarization mode.

- Conservation of 4-momentum in weakly-dispersive vacuum (linear polarization tensor) yields Adler's (1971) selection rule: *only* $\perp \rightarrow \parallel\parallel$ is a permitted mode.
- Splitting attenuation at near critical fields is 100% polarized, with \perp turnover at lower energies (c.f. pair creation).

Photon Splitting Rates



- Rate calculated originally by Adler (1971); see also Papayan & Ritus (1972); Stoneham (1979), Baier et al. (1986); Weise et al. (1998); Baring (2000).

Photon Splitting in Photospheres

- Splitting shuts off at 100-150 keV when $B > 1$. This sets a natural scale for calibrating flare spectra (e.g. Baring & Harding 1995);
- Lower frequency photons Comptonize, higher energy ones split (biasing $||$ state).
- Mode conversion character for the two processes is opposite, generating distinctive spectropolarimetric signatures.

SGR 1900+14 Outburst light curves and spectrum (Jun-Aug 1992)

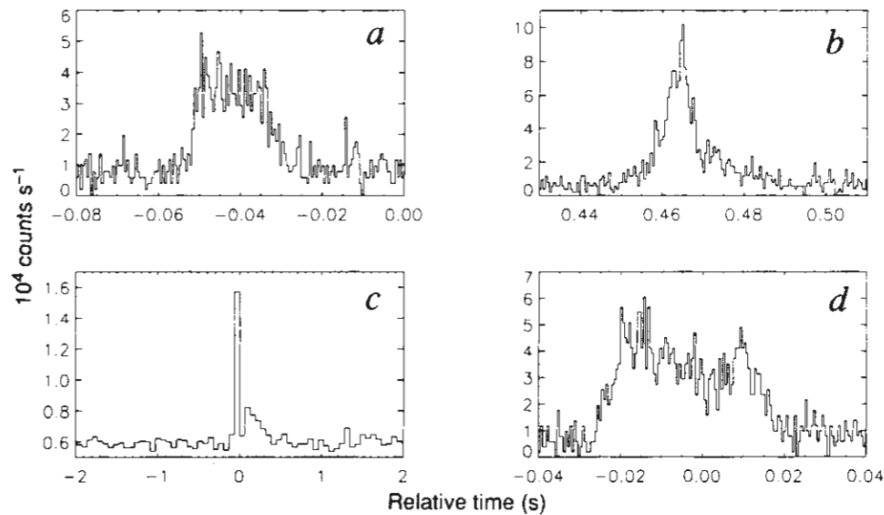


FIG. 1 Light curves of the three SGR bursts detected with the Burst and Transient Source Experiment (BATSE) on the Compton Gamma Ray Observatory. BATSE is unique in combining good sensitivity to weak γ -ray and SGR-like bursts with the capability of determining their locations in a single experiment. *a, b*, First and second pulse, respectively, of the 19 June 1992 trigger. The counts are integrated between 20 and 100 keV. Time resolution is 0.512 ms. *c*, Event of 8 July 1992 recorded with 64-ms time resolution (the only resolution available). The initial spike of <64 ms appears only up to 100 keV. *d*, Event of 19 August 1992 recorded with 0.512-ms resolution between 20 and 100 keV. Notice the similarity in structure between *a* and *d*.

NATURE · VOL 362 · 22 APRIL 1993

■ Kouveliotou et al. (1993)

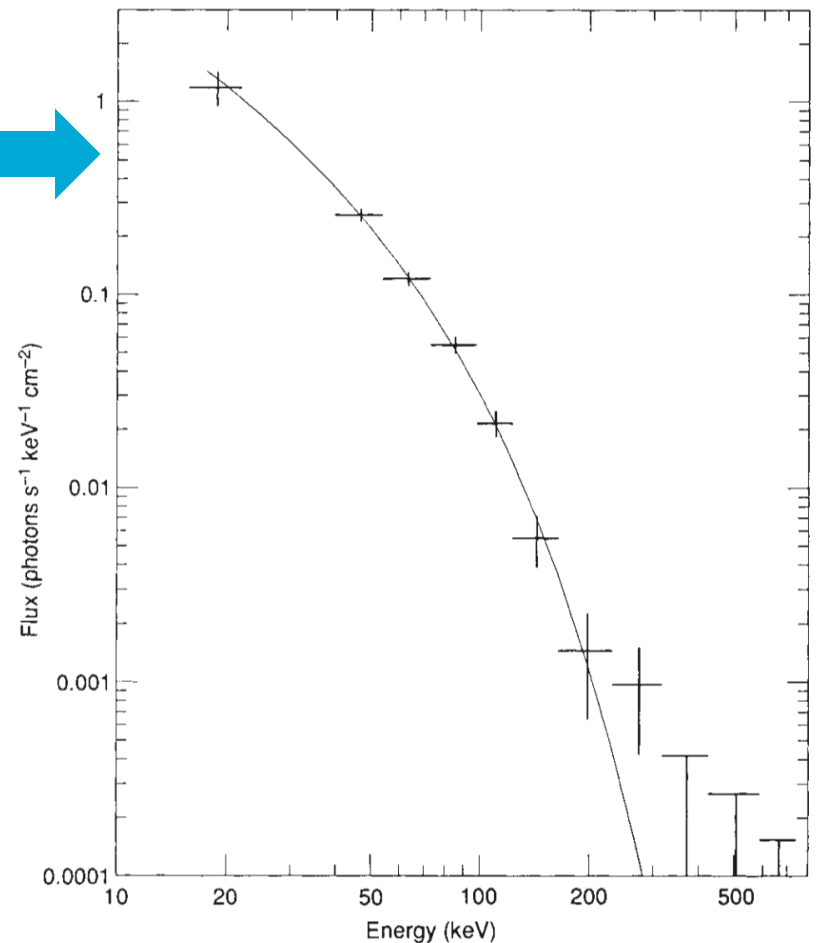


FIG. 2 Photon spectrum of the pulse of Fig. 1*b*. The spectrum is integrated over 32 ms and corresponds to the peak of the pulse. The gap in the spectrum between ~ 20 and 40 keV is due to a period of telemetry failure during transmission of the data. The curve indicates the best-fit OTTB function, of the form $A \exp(-E/KT)/E$, with $kT = 39 \pm 3$ keV.

Conclusions

- Magnetar flare spectral formation controlled by Comptonization and photon splitting in photospheric equatorial region;
- Pair creation probably active, but hard to diagnose;
- Hard initial spikes may involve relativistic Compton upscattering and pair production, perhaps mimicking GRB outflows to some extent?
- Expect strong and distinctive polarization signatures for giant flare tails and X-class magnetar flares;
- **Future agendas:** dig deep - Compton polarimeters with sensitivity throughout tail pulse profile can probe photospheric physics and geometry:
 - GEMS at too low an energy, and is a pointing telescope;
 - Need an all-sky monitor in Compton band (e.g. POET);
 - Detailed modeling of phase-resolved spectra with polarizations in photospheric bubbles is needed.